Alpha-chain states in ^{12}C

G.S. Anagnostatos*
Department of Physics, University of Oxford, Nuclear Physics Laboratory, Keble Road, Oxford, OX1 3RH United Kingdom
(Received 4 March 1994)

Alpha-chain states in ^{12}C are studied by employing the isomorphic shell model. Where possible α particles and their spatial distribution are derived, instead of being assumed as usual in α-cluster models. It has been found that the average forms of both the ground state and the first 0^+ excited state can be associated with an α chain composed of three α particles in a row. The ground state and the first 0^+ excited state energies and their rotational bands, together with their charge radii and intrinsic quadrupole moments, have been computed and compared with the predictions of α-particle models. With reference to experimental data, all quantities examined lend support to the present approach.

PACS number(s): 21.60.Gx, 25.70.Ef, 27.20.+n

I. INTRODUCTION

The α-cluster model and its variations have a long history in nuclear physics and many geometries of α-cluster configurations have been examined in the literature [1–11] ranging from three-dimensional high-symmetry shapes of a tetrahedron [8] (e.g., in ^{16}O) or an octahedron [7] (e.g., in ^{24}Mg) to two-dimensional configurations [6,12] (e.g., in ^{12}C) and even to completely linear arrangements [6,13] (e.g., in α-chain states of $4N$ nuclei) counting from two (in the case of ^{8}Be) up to seven [12] (in the case of ^{28}Si) α particles in a row.

The geometries in the α-cluster models arise through the long-range effects of antisymmetrization and the mean field combined with a preference for simple underlying structures [6,14]. Calculations in the cranked α-cluster model [11] and in the Nilsson-Strutinsky model [15] indicate that shell nonuniformities in single-particle spectrum play a vital role in determining the stability and shapes of α-cluster configurations [16].

The α-cluster model, despite some initial successes, appeared in general unable to predict the properties of nuclei heavier [7,10] than ^{20}Ne. However, this specific deficiency has been overcome and the results obtained are comparable to those from Hartree-Fock calculations by avoiding artificial constraints to be imposed on the symmetry of the mean positions of the α clusters [10].

The common characteristic of many α-cluster models is that the α particles involved in the nuclear structure are considered preformed and thus the nucleus appears in the framework of these models as an aggregate of α-particle subunits. Despite the apparent successes of these models, however, the wealth of nuclear reactions does not support this α-particle composition of nuclei even for the $4N$ nuclei. One thus could compromise the situation by assuming that each such α particle is composed of four close-by nucleons (two neutrons and two protons) with the same n and l quantum numbers instead of being composed of four nucleons in s state as usually assumed. That is, even in the Bloch-Brink model, the alpha particles may also dissolve into nucleons since, for cluster separations reaching zero, antisymmetrization forces the cluster wave function into some shell-model limit. This would also be consistent with the relaxation of the α-cluster positions [10] mentioned earlier. Thus, effectively nucleons and not α particles could be the fundamental constituents of a nucleus.

In the present study an alternative approach is considered where indeed nucleons and not α particles compose the nuclei and thus possible α particles and their spatial distributions in nuclei are derived. Specifically, the semiclassical [17] part of the isomorphic shell model is employed. The semiclassical instead of the quantum-mechanical part [18] of the model is utilized since this part is closer to the α-cluster models and thus a comparison between them is easier and more comprehensive. An outline of the model is given in the next section. Here, only a very brief comparison is attempted for the geometry involved in this model and that in the main α-cluster model [6,7] of Bloch and Brink. In the second case, several geometries are chosen for a particle nucleus based on symmetry arguments for the α particles involved and then the binding energy is used for the final selection of geometry. In the first case a common geometry for all nuclei is derived by packing the nuclear shells whose average forms result from the independent particle assumption. The part of this geometry utilized by the nucleons of a specific nucleus results from the search for the maximum binding energy.

II. THE ISOMORPHIC SHELL MODEL

The isomorphic shell model is a microscopic nuclear-structure model that incorporates into a hybrid model

*Permanent address: Institute of Nuclear Physics, National Center for Scientific Research Demokritos, Aghia Paraskevi, Attiki, 15310 Greece.

the prominent features of single-particle and collective approaches in conjunction with the nucleon finite size [17,18]. The single-particle component of the model is along the lines of the conventional shell model with the *only* difference that in the model the nucleons creating the central potential are the nucleons of each particular nuclear shell alone, instead of all nucleons in the nucleus as assumed in the conventional shell model [18]. That is, our Hamiltonian is analyzed into partial state-dependent Hamiltonians for neutrons (N) and for protons (Z) as follows, where crossing terms between partial Hamiltonians of different shells have been omitted:

$$\begin{aligned} H &= {}_N H + {}_Z H \\ &= {}_N H_{1s} + {}_N H_{1p} + {}_N H_{1d2s} + \cdots \\ &\quad + {}_Z H_{1s} + {}_Z H_{1p} + {}_Z H_{1d2s} + \cdots . \end{aligned} \tag{1}$$

While a finite square-well or Woods-Saxon potential would be a more realistic choice of the potential, for reasons of simplicity, we take the harmonic-oscillator (HO) potential without spin-orbit coupling, where the expressions of the mean-square radius and of the energy eigenvalues, necessary in demonstrating the model, are exceptionally simple and have closed mathematical forms. In addition, the appearance of the finite negative constants $-{}_N V_i$ and $-{}_Z V_i$ in the neutron and the proton harmonic-oscillator potentials below reduces the startling impression given when an infinite potential is used for determining total binding energies.

Thus, for each partial neutron or proton Hamiltonian we take

$${}_N H_i = {}_N V_i + {}_N T_i = -{}_N \bar{V}_i + \tfrac{1}{2} m ({}_N \omega_i^2) r^2 + {}_N T_i , \tag{2}$$

$${}_Z H_i = {}_Z V_i + {}_Z T_i = -{}_Z \bar{V}_i + \tfrac{1}{2} m ({}_Z \omega_i^2) r^2 + {}_Z T_i . \tag{3}$$

That is, each harmonic-oscillator potential has its own state-dependent frequency ω. These ω are *not* taken as adjustable parameters, but all are determined from the harmonic-oscillator relation [19]

$$\hbar\omega = \left(\frac{\hbar^2}{m \langle r^2 \rangle} \right) \left(n + \frac{3}{2} \right) , \tag{4}$$

where n is the harmonic-oscillator quantum number and $\langle r^2 \rangle^{1/2}$ is the average radius of the relevant high fluximal shell determined by the semiclassical part of the model specified below.

The solution of the Schrödinger equation with Hamiltonian (1), in spherical coordinates, is

$$\Psi_{nlm}(r, \theta, \phi) = R_{nl}(r) Y_l^m(\theta, \phi) , \tag{5}$$

where $Y_l^m(\theta, \phi)$ are the familiar spherical harmonics and the expressions for the $R_{nl}(r)$ are given in several books of quantum mechanics and nuclear physics, for example, see Table 4-1 of Ref. [19].

The only difference between our wave functions and those in these books is the different ω's as stated in (2) and (3) above. Those of our wave functions, however, which have equal l value, because of the different $\hbar\omega$, are not orthogonal, since in these cases the orthogonality of Laguerre polynomials does not suffice. Orthogonality, of course, can be obtained by applying established procedures, e.g., the Gram-Schmidt process.

According to Hamiltonian (1), the binding energy of a nucleus with A nucleons in the case of orthogonal wave functions takes the simple form given by (6)

$$E_{\mathrm{BE}} = \tfrac{1}{2} (\bar{V} A) - \tfrac{3}{4} \left[\sum_{i=1}^{A} \hbar\omega_i (n + \tfrac{3}{2}) \right] , \tag{6}$$

where $\bar{V}$ is the average potential depth [18]. The coefficients $\frac{1}{2}$ and $\frac{3}{4}$ take care of the double counting of nucleon pairs in determining the potential energy.

Applications and details of the quantum-mechanical part of the model are given in Ref. [18]. Here an application of the semiclassical part (see Refs. [17,20–25]) in the place of the quantum-mechanical part of the model is considered in the spirit of Ehrenfest's theorem [26], which for the observables of position ($\mathbf{R}$) and momentum ($\mathbf{P}$) takes the form

$$\frac{d}{dt} \langle R \rangle = \frac{1}{m} \langle P \rangle , \tag{7}$$

$$\frac{d}{dt} \langle P \rangle = -\langle \nabla V(R) \rangle . \tag{8}$$

The quantity $\langle R \rangle$ represents a set of three time-dependent numbers $\{\langle X \rangle, \langle Y \rangle, \langle Z \rangle\}$ and the point $\langle R \rangle(t)$ is the center of the wave function at the instant t. The set of those points which correspond to the various values of t constitutes the trajectory followed by the center of the wave function.

From (7) and (8) we get

$$m \frac{d^2}{dt^2} R = -\langle \nabla V(R) \rangle . \tag{9}$$

Furthermore, it is known that, for the *special* case of the harmonic-oscillator potential assumed by the isomorphic shell model in (3), the following relationship is valid:

$$\langle \nabla V(R) \rangle = [\nabla V(r)]_{r = \langle R \rangle} , \tag{10}$$

where

$$[-\nabla V(r)]_{r = \langle R \rangle} = F . \tag{11}$$

That is, for this potential the average of the force over the whole wave function is rigorously equal to the classical force F at the point where the center of the wave function is situated. Thus, for the special case (harmonic oscillator) considered, the motion of the center of the wave function precisely obeys the laws of classical mechanics. Any difference between the quantum and the classical description of the nucleon motion exclusively depends on the degree the wave function may be approximated by its center. Such differences will contribute to the magnitude of deviations between the experimental data and the pre-

dictions of the semiclassical part of the model employed here.

Thus, in the semiclassical treatment the nuclear problem is reduced to that of studying the centers of the wave functions presenting the constituent nucleons or in other words, of studying the average positions of these nucleons. For this study the following two assumptions are employed in the isomorphic shell model: (i) The neutrons (protons) of a closed neutron (proton) shell, considered at their *average* positions, are in *dynamic equilibrium* on the sphere representing the average size of that shell. (ii) The average sizes of the shells are determined by the *close packing* of the shells themselves, provided that a neutron and a proton are represented by *hard spheres* of definite sizes (i.e., $r_n = 0.974$ fm and $r_p = 0.860$ fm). It is apparent that assumption (i) is along the lines of the conventional shell model, while assumption (ii) is along the lines of the liquid-drop model.

The model employs a specific equilibrium of nucleons, considered at their average positions on concentric spherical cells, which is valid whatever the law of nuclear force may be: assumption (i). This equilibrium leads uniquely to Leech [27] (equilibrium) polyhedra as average forms of nuclear shells. All such nested polyhedra are closed packed, thus taking their minimum size: assumption (ii). The cumulative number of vertices of these polyhedra, counted successively from the innermost to the outermost, reproduce the magic numbers each time a polyhedral shell is completed [17] (see the numbers in the brackets in Fig. 1 there and in this paper).

To conceptualize the isomorphic shell model, it should first be related to the conventional shell model. Specifically, the main assumption of the simple shell model, i.e., that each nucleon in a nucleus moves (in an average potential due to all nucleons) independently of the motion of the other nucleons, may be understood here in terms of a *dynamic equilibrium* in the following sense [17]. Each nucleon in a nucleus is *on average* in a *dynamic equilibrium* with the other nucleons and, as a *consequence*, its motion may be described independently of the motions of the other nucleons. From this, one realizes that dynamic equilibrium and independent particle motion are *consistent* concepts in the framework of the isomorphic shell model.

In other words, the model implies that at some instant in time (reached *periodically*) all nucleons could be thought of as residing at their individual average positions, which coincide with the vertices of an equilibrium polyhedron for each shell. This system of particles evolves in time according to each independent particle

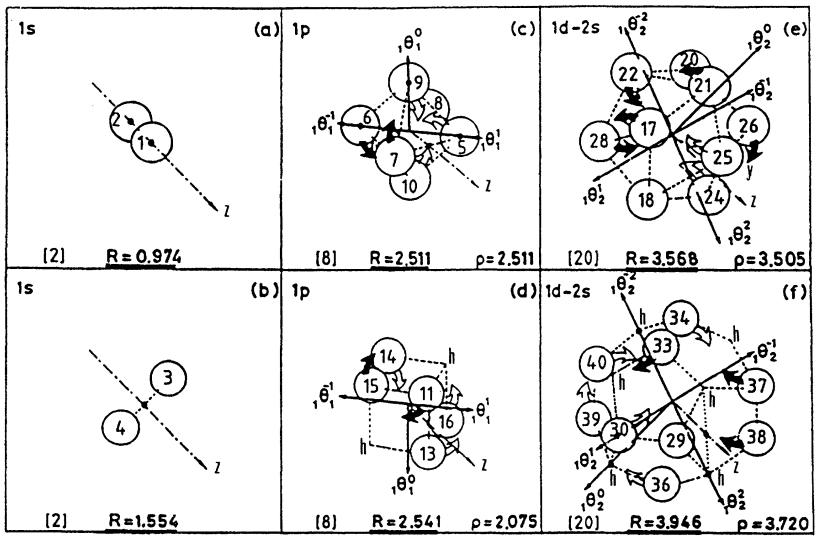

FIG. 1. The isomorphic shell model for the nuclei up to $N = 20$ and $Z = 20$. The high-symmetry polyhedra in row 1 (i.e., the zerohedron, the octahedron, and the icosahedron) stand for the average forms for neutrons of (a) the $1s$, (c) the $1p$, and (e) the $1d2s$ shells, while the high-symmetry polyhedra in row 2 [i.e., the zerohedron, the hexahedron (cube), and the dodecahedron] stand for the average forms of (b) the $1s$, (d) the $1p$, and (f) the $1s2s$ shells for protons. The vertices of polyhedra stand for the average positions of nucleons in definite quantum states (τ, n, l, m, s). The letters h stand for the empty vertices (holes). The z axis is common for all polyhedra when these are superimposed with a common center and with relative orientations as shown. At the bottom of each block the radius R of the sphere exscribed to the relevant polyhedron and the radius ρ of the relevant classical orbit, equal to the maximum distance of the vertex state (τ, n, l, m, s) from the axis ${}_n\theta_l^m$ precisely representing the orbital angular-momentum axis with definite n, l, and m values, are given. Curved arrows shown help the reader to visualize for each nucleon round what axis is rotated, where solid (open) arrows show rotations directed up (down) the plane of the paper. All polyhedra vertices are numbered as shown. The backside (hidden) vertices of the polyhedra and the related numbers are not shown in the figure.

motion. This is possible, since axes standing for the angular-momenta quantization of directions are *identically* described by the rotational symmetries of the polyhedra employed [28–31]. For example, see Ref. [30], where one can find a complete interpretation of the independent particle model in relation to the symmetries of these polyhedra. Such vectors are shown in Fig. 1 for the orbital angular-momentum quantization of directions involved in all nuclei up to $N = 20$ and $Z = 20$.

Since the radial and angular parts of the polyhedral shells in Fig. 1 are well defined, the coordinates of the polyhedral vertices (nucleon average positions) can be easily computed. These coordinates up to $N = Z = 20$, needed here for the application of the model on ^{12}C (see next section), are already published in footnote 14 of Ref. [20], and in footnote 15 of Ref. [21]. These coordinates correspond to the relevant R values of the exscribed polyhedral spheres given in Fig. 1 (see bottom line at each block).

According to the isomorphic shell model, the average positions of nucleons in a nucleus are distributed at the vertices of the polyhedral shells as shown, for example, in Fig. 1. The specific vertices occupied, for a given (closed- or open-shell) nucleus at the ground state, form a vertex configuration (corresponding to a state configuration) that possesses a maximum binding energy (BE) in relation to any other possible vertex configuration. This maximum BE vertex configuration defines the average form and structure of the ground state of this nucleus. All bulk (static) ground-state properties of this nucleus (e.g., BE, rms radii, etc.) are derived as properties of this structure, as has been fully explained in Ref. [17] and will become apparent below.

The quantities estimated by the model in the framework of its semiclassical part [17,20,22] (see the next section) are potential energy V_{ij}, Coulomb energy $(E_C)_{ij}$; average kinetic energy $\langle T\rangle_{nlm}$; odd-even energy E_δ; binding energy $E_{\rm BE}$; collective rotational energy $E_{\rm rot}$; rms charge, mass, and effective radii $\langle r^2\rangle^{1/2}$; and electric quadrupole moment by using (12)–(22);

$$V_{ij} = (1.7\times 10^{17})\frac{e^{-(31.8538)r_{ij}}}{r_{ij}} - 187\frac{e^{-(1.3538)r_{ij}}}{r_{ij}} , \quad (12)$$

where the internucleon distances r_{ij} are estimated following Fig. 1 or (the same) the corresponding coordinates of polyhedral vertices [20,21];

$$(E_C)_{ij} = \frac{e^2}{r_{ij}} , \quad (13)$$

where the distances r_{ij} are computed as explained above;

$$\langle T\rangle_{nlm} = \frac{\hbar^2}{2M}\left[\frac{1}{R^2_{\rm max}} + \frac{l(l+1)}{\rho^2_{nlm}}\right] , \quad (14)$$

where $R_{\rm max}$ is the outermost polyhedral radius (R) plus the relevant nucleon radius (i.e., $r_n = 0.974$ fm or $r_p = 0.860$ fm), i.e., the radius of the nuclear volume in which the nucleons are confined, M is the nucleon mass, ρ_{nlm} is the distance of the vertex (n,l,m) from the axis ${}_n\theta_l^m$ (see Fig. 1 and Ref. [22]);

$$E_{\rm BE} = -\sum_{\text{all nucleon pairs}} V_{ij} - \sum_{\text{all proton pairs}} \frac{e^2}{r_{ij}} - \sum_{\text{all nucleons}} \langle T\rangle_{nlm} - E_\delta + E_{\rm rot} , \quad (15)$$

where distances r_{ij} are estimated as above and E_δ is a correction "odd-even" term familiar from the liquid-drop model. Here the E_δ value is equal to zero for even-Z even-N nuclei for which the potential in (12) is exclusively derived [20] and thus no correction is needed, while for odd-A nuclei its value is taken equal [19] to $80/A$ MeV, i.e.,

$$E_\delta = \frac{80}{A} ; \quad (16)$$

$$E_{\rm rot} = \frac{\hbar^2 I(I+1)}{2J} , \quad (17)$$

where J is the moment of inertia of the rotating part of the nucleus given by (18)

$$J = \sum_i m\rho_i^2 = mN_{\rm rot}\langle r^2\rangle_{\rm rot} , \quad (18)$$

where $N_{\rm rot}$ is the number of nucleons participating in the collective rotation and $\langle r^2\rangle_{\rm rot}$ is the rms radius of these nuclei.

The term $E_{\rm rot}$ in (15) is meaningful for the ground state *only* for the cases where the angular speed ω due to independent particle motion is comparable (about equal) to that due to collective motion in such a way that these two motions are coupled even at the ground state, i.e., for these cases the adiabatic approximation is not valid;

$$\langle r^2\rangle_m^{1/2} = \left[\frac{\sum_{i=1}^Z R_i^2 + \sum_{i=1}^N R_i^2 + Z(0.8)^2 + N(0.91)^2}{Z+N}\right]^{1/2} , \quad (19)$$

$$\langle r^2\rangle_{\rm ch}^{1/2} = \left[\frac{\sum_{i=1}^Z R_i^2}{Z} + (0.8)^2 - (0.116)\frac{N}{Z}\right]^{1/2} , \quad (20)$$

where the subscripts ch and m refer to charge and mass, R_i is the radius of the ith proton or neutron average position from Fig. 1, Z and N are the proton and the neutron numbers of the nucleus, 0.8 and 0.91 fm are the rms radii of a proton and of a neutron, and -0.116 fm^2 is the mean square charge radius of a neutron [32]. The 0.91 fm value for a neutron is taken from the 0.8 fm value for a proton by considering proportionality according to the sizes of their bags 0.974 and 0.860 fm, respectively, i.e., 0.91=0.8(0.974/0.860);

$$\langle r^2\rangle_{\rm eff}^{1/2} = [\langle r^2\rangle_m + \langle r^2\rangle_{\rm rot}]^{1/2} ; \quad (21)$$

$$eQ'_{\text{intr}} = \sum_i eQ'_i = e\sum_{i=1}^{Z} R_i^2(3\cos^2\theta_i - 1) \ , \qquad (22)$$

where Q' stands for the intrinsic quadrupole moment, R_i is the radius of the ith proton average position, and θ_i is the corresponding azimuthal angle with respect to the symmetry axis.

III. CALCULATIONS AND DISCUSSION

In the α-cluster model of the nucleus referring to α-chain states, ^{12}C ($N = 3$) is the key nucleus since an α-chain structure for ^{8}Be ($N = 2$) is apparent and since the appearance of such structure for heavier nuclei ($N \geq 4$) could be associated to ^{12}C structure particularly if the α-chain states of these heavier nuclei could be thought of as forming molecular structures of the type ^{12}C+$(N-3)\alpha$, either ^{12}C+^{8}Be or ^{12}C+^{12}C. Thus in the following we will concentrate on ^{12}C.

The average structure of ^{12}C, in the framework of the isomorphic shell model, comes from Fig. 1 by considering the states ($1s$ and $1p_{3/2}$) involved in this nucleus. Specifically, from Fig. 1 the average nucleon positions numbered 1 and 2 (for $1s$ neutrons), 3 and 4 (for $1s$ protons), 5–8 (for $1p_{3/2}$ neutrons), and 11–14 (for $1p_{3/2}$ protons) are depicted as shown in Fig. 2(a) by employing the same numbers. Thus, Fig. 2(a) contains part of Fig. 1 and so, as mentioned, all coordinates of the average nucleon positions involved are known [20,21]. Further, Fig. 2(b) is almost identical to Fig. 2(a) and only slightly differs with respect to the average positions of the two $1s$ protons (3 and 4). Specifically, due to the absence of $1p_{1/2}$ neutrons in ^{12}C (9 and 10) whose average positions together with those of $1p_{3/2}$ neutrons (5–8) determine the symmetry of the average positions for the $1s$ protons, these two latter positions can relax getting closer to the average positions for the $1p_{3/2}$ neutrons (5–8) in such a way that their corresponding nucleon bags come in contact. Thus, the difference between Fig. 2(b) and Fig. 2(a) is visualized from the contact (or not) of the bags numbered 3 and 4 with the bags numbered 5 and 8, and 6 and 7, respectively. This relaxation of the two proton average positions leads to larger binding energy for ^{12}C.

Furthermore, in the model each set of the following four nucleon average positions numbered (1–4), (5,7,11,13), and (6,8,12,14) consists of two protons and two neutrons with the same n and l quantum numbers which are close together for the instant depicted by Figs. 2(a) and (b). Thus, in the model each of these three sets can be considered as an α particle. Considering now the center of gravity for each of these α particles Fig. 2(c) results, where indeed these three α-like particles are in a row forming a linear chain. For later moments, of course, each of the four nucleons composing any one of the above three α-particle-like structures will evolve by following its independent particle motion. That is, each nucleon will rotate in an orbital round its own axis of orbital angular momentum vector as schematically shown by arrows in Fig. 1.

In the framework of the isomorphic shell model now the observables of rms charge radius and of binding energy can be estimated. Specifically, from Eq. (20) since all R_i involved in Figs. 2(a) and (b) are known [17] [namely, $R_{1s\ \text{protons}} = 1.544$ fm, and $R_{1p\ \text{protons}} = 2.541$ fm; see Figs. 1(b) and (d)], the charge rms radius is computed equal to 2.37 fm for each of Figs. 2(a) and (b) ($\langle r^2\rangle^{1/2}_{\text{ch,expt}} = 2.37$ fm). Also, from Eqs. (12)–(15) since all coordinates of the nucleon average positions [20,21] and the radial distances involved in Figs. 2(a) and (b) [namely in fm, $R_{\max} = 2.511 + 0.974$, $\rho_{1p\ \text{proton}} = 2.075$, $\rho_{1p\ \text{neutron}} = 2.511$, also $E_{\text{rot}} = 0$; see Figs. 1(c) and (d)] are known [20,21], the binding energy for Figs. 2(a) and(b) are computed equal to 86.0 and 94.2 MeV, respectively.

Figures 2(a) and (b) have been found to be the two average-nucleon-position configurations with the largest binding energies with respect to any other possible con-

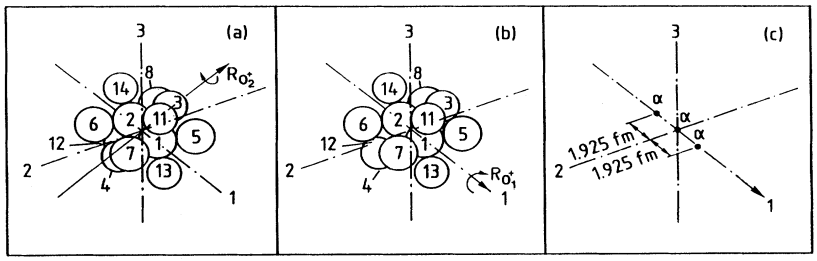

FIG. 2. Average forms for ^{12}C, according to the isomorphic shell model, composed of the average positions of the constituent nucleons. (a) stands for the first 0^+ excited state at 7.65 MeV and (b) for the ground state. Average nucleon positions are numbered as shown by using for the same position the same number as in Fig. 1. Thus, one can observe that for the positions shown in Figs. 1(a)–(d) those numbered (9) and (10) for neutrons and (15) and (16) for protons are the only not present in Fig. 2. (c) comes from either Fig. 1(a) or Fig. 1(b) when each of the three sets of four close-by nucleons (two neutrons and two protons) of same n and l numbered (1–4), (5,7,11,13), and (6,8,12,14) are assumed forming a sort of an α particle. Axes labeled 1,2, and 3 stand for C_2 symmetry axes and those labeled $R_{0_1^+}$ and $R_{0_2^+}$ for rotational axes referring to the first (0_1^+) and to the second (0_2^+) 0^+ levels.

figuration for ^{12}C involving s and p or even d states and coming from Figs. 1(a)–(f). Thus, Fig. 2(b) is associated with the ground state and Fig. 2(a) with the 7.653±0.3, $J^\pi = 0_2^+$ excited state [34] of ^{12}C possessing 92.2 and 84.55 MeV experimental binding energies [33], respectively. The intermediate excited state [34] at 4.4392±0.3, $J^\pi = 2_1^+$, will be discussed shortly. Center-of-mass corrections are not included.

It is satisfying that the present predictions are close to the experimental values for the binding energies but also for the radii [35]. The comparison is even more to our favor if we consider the corresponding α-model predictions [7] given in Table I. However, a more detailed comparison with α-cluster models will be made later.

As seen from Figs. 2(a) and (b), the deformation of the average shapes for the ground state and the 0_2^+ excited state of ^{12}C is apparent. In these figures the axes of symmetry and the corresponding axes of rotation are also shown. Specifically, the axis of rotation labeled $R_{0_1^+}$ is perpendicular to both axes of symmetry labeled 2 and 3, while the axis of rotation labeled $R_{0_2^+}$ is defined from the proton-average positions 3 and 4 and is perpendicular to the axis of symmetry labeled 1. At this point, of course, a clarification of the terminology concerning symmetry and rotation axes in Fig. 2 should be made.

Axes 1 and 2 are axes of symmetry in both Figs. 2(a) and (b) after considering the fact that the proton-average positions 3 and 4 cannot be distinguished from their symmetric counterpart average positions (i.e., from the positions 3′ and 4′ not shown in these figures for reasons of simplicity). Both Figs. 2(a) and (b) have a triaxial structure, since their axes of symmetry labeled 1–3 refer to a discrete C_2 (i.e., 180°) symmetry. That is, none of these axes has the C_∞ symmetry appearing, e.g., in an axially symmetric ellipsoidal. Thus, quantum-mechanical rotation around the C_2 symmetry axis 1 (labeled $R_{0_1^+}$) is permissible. However, at first glance Fig. 2(c) gives the impression that axis 1 has C_∞ symmetry and thus no rotation round this axis is quantum mechanically permissible. This false impression comes from the fact that in Fig. 2(c), in order to facilitate the comparison of this work with the α-cluster models, α particles are presented by points standing for their center of gravity. The correct reading of the figure is to consider the distribution of the nucleons constituting these α particles as has indeed been considered in the calculations of all observables in the present work. This difference in nucleon distribution makes the difference between Figs. 2(a) and (b), even if the α-cluster separation [see Fig. 2(c)] is the same for both figures.

Since all coordinates involved in Figs. 2(a) and (b) are known [20,21], by applying Eq. (18) the relevant moments of inertia are estimated. Namely, $J_a = 43.6M$ fm^2 and $J_b = 28.03M$ fm^2, where M stands for the nucleon mass and the contribution to the moment of inertia coming from the finite nucleon size has been empirically incorporated equal to $0.165M$ fm^2 for each nucleon participating in the collective rotation.

By assuming no variation of the moment of inertia with angular momentum and by applying Eq. (17) the bands corresponding to the rotational axes labeled $R_{0_1^+}$ and $R_{0_2^+}$ are those given in Table II.

The second band is what is usually considered by the α-cluster models [7] as corresponding to the linear α-chain states for ^{12}C. Of course, the existence of such a band is not clearly supported by the experimental data [34]. Its existence exclusively depends on whether in the future the J^π for the state 10.3±3 MeV will be found to be 2^+

TABLE I. Theoretical predictions and experimental values for the ground state (0_1^+) and first 0^+ excited state (0_2^+) of ^{12}C.

Approach	J^π		Energy (MeV)		rms charge radius (fm)		Intrinsic quadrupole moment (fm^2)	
Experiment	0_1^+		92.2[b]		2.37[e]		±21[d]	
	0_2^+			7.65				
Isomorphic	0_1^+ (chain)		94.2		2.37		21	
Shell model	0_2^+ (chain)			8.2		2.37		21
α particle	0_1^+ (triangle)	V1	72.7					
Model[a]		V2	64.3					
With forces		B1	62.0		2.62		−43[f]	
V1, V2, B1	0_2^+ (chain)	V1		15.0		3.27[e]		
		V2		8.7				
		B1		6.1				

[a]See Ref. [7].
[b]See Ref. [34].
[c]See Ref. [35].
[d]See Ref. [37].
[e]See Ref. [38].
[f]See text (Sec. III) for other calculated values (e.g. −21.6 fm^2). The value listed here is in fact that of the mass quadrupole moment, even if this is not clearly stated in Ref. [7].

TABLE II. Rotational ground state and 0_2^+ excited bands of ^{12}C.

Band	J^π	J^π	Experiment[a] Energy (MeV)	Isomorphic Shell model (MeV)	Isomorphic α-particle models[b] (MeV)
	2^+	2^+	4.44	4.28	2.76[c]
0_1^+	4^+ (4^+)		14.08	14.28	
	6^+		28.9	29.98	
	0^+	0^+	7.65	7.65	7.65
0_2^+	2^+ (0^+)		10.3	10.5	8.90
	4^+			17.2	12.1

[a]See Ref. [34].
[b]See Ref. [39].
[c]See Ref. [38].

in place of the present tentative [34] assignment (0^+).

What is really different between the present approach and the α-cluster models is the nature of the first band, i.e., of the ground-state band in Table II. In these models α particles are arranged at the corners of an equilateral triangle [7] for the ground state of ^{12}C. Such a triangular configuration of α particles round the nuclear center is based on the assumption that the α particle is a fundamental constituent of ^{12}C nucleus. In such a case by considering any reasonable α-α interaction, the most compact structure (and thus with maximum binding energy) is that of an equilateral triangle and should be assigned to the ground state of ^{12}C. In the framework of the present model, however, nucleons and not α particles are the constituents of any nucleus and it is the Pauli principle together with the maximum binding energy which determine what average nucleon positions are occupied and eventually what is the average shape of a specific nucleus. The good agreement between the experimental data and the predictions of the present model concerning the member states of the ground-state band [34] lend support to the present approach, where a linear instead of a triangular average shape for the ground state of ^{12}C is employed.

Finally, an estimation of the electric quadrupole moment of ^{12}C is made which constitutes a very sensitive test of the angular distribution of the average structure for any nucleus. Dealing with average values, the intrinsic quadrupole moment is given [19] by (22), where for Fig. 2(b) representing the ground state of ^{12}C each R_i has been specified [17] above (see R values in Fig. 1) and the corresponding θ_i is the azimuthal angle for the proton average position i with respect to the axis 1 (see Fig. 2), which is the quantization axis for all vectors presenting quantization of direction [28–32] for orbital angular momenta shown in Fig. 1 and the symmetry axis for the estimation of $Q'_{\rm intr}$ (namely [36], $\theta_{3,4} = 90°$ and $\theta_{11-14} = 35°\ 15'52''$). It is satisfying that the resulting value $Q'_{\rm intr} = 21.0$ fm^2 is identical to the measured [37] absolute value of the intrinsic quadrupole moment. The corresponding value coming from the α-cluster model [7] used for the construction of Table I is -43 fm^2, while more recent calculations [40,41] give -21.6 fm^2 and [41] -21.7 fm^2. Hence, the difference between the present model and the Bloch-Brink model concerning the electric quadrupole moment essentially lies in the sign of the $Q'_{\rm intr}$.

IV. CONCLUSIONS

In the present study of ^{12}C the isomorphic shell model [17,18] has been employed as a cluster approach to atomic nuclei, where consideration of the nucleon finite size [17] constitutes one of the main features of the model. This feature allows the packing and clusterization in a nucleus [17]. What are really packed in the model are the shells themselves [17] taken as entities. Thus, only nucleons necessary for the shell packing are in contact. That is, the model does not support general packing of nucleons which should lead to much higher density. It is satisfying that this packing of shells reproduces a magic number [17] each time a saturated shell is added into the packing. The close reproduction of binding energies and sizes in many nuclei by both the quantum [18] and semiclassical [17] parts of the model lends support to the present approach and makes its results reliable.

A prolate average shape with a sizable positive intrinsic quadrupole moment is predicted for ^{12}C which can be considered as a linear chain of three α particles, when each two close-by pairs of neutrons and protons with the same n and l quantum numbers (like an α particle) are presented by their center of gravity. Such a linear α chain has already been predicted by α-cluster models [7]. However, here the α chain stands for *both* the excited 0_2^+ state [34] at 7.65 MeV (as in these models) and the ground state (instead of an equilateral triangle in these models [7]). The good agreement with experimental values for all observables examined, superior to those from α-cluster models, support the credibility of the present approach. Of course, the difference in the sign of the deformation for the ground state between the predictions of the present model and those of the α-cluster models cannot be ignored. However, despite much effort the quantitative experimental evidence is inconclusive [42]. Most of it derives from model-dependent analysis of electron scattering and hadron scattering data. Some of these analyses are inherently insensitive to the sign of the deformation and there are indications that the values obtained are projectile dependent and also that the findings strongly depend on the assumption that the nuclear charge distribution is spheroidal [42]. Furthermore, in support of our findings (that 0_1^+ and 0_2^+ states in ^{12}C have the same sign of deformation) there are rather recent calculations [43,44] on the basis of the Brink-type 3α model which show that the rather strong $0_2^+ \to 0_1^+$ monopole and $0_2^+ \to 2_1^+$ $E2$ transitions are hardly explained unless a mixture of the equilateral triangle and linear 3α-chain geometries are assumed both for the 0_1^+ and 0_2^+ states [40].

The above conclusions are further strengthened by the fact that the isomorphic shell model used here employs no adjustable parameters. It uses, of course, two numerical parameters for the sizes of neutron and proton bags [17,22] and four parameters for the two-body potential [20] employed, but these six parameters are universal parameters of the model and are constant for all properties in all nuclei. In the present approach no *ad hoc*

assumption has been made and all predictions are based on the isomorphic shell model, all of whose parameters necessary for its implementation have been published independently a long time ago.

ACKNOWLEDGMENTS

I want to express my deep appreciation to Dr. P. E. Hodgson of the Nuclear Physics Laboratory (University of Oxford) for his valuable help in all stages of this research. Also, it is my pleasure to thank Dr. A. C. Merchant of the Nuclear Physics Laboratory (University of Oxford) for valuable discussions and for critical reading and suggestions concerning the present work. Finally, I want to thank the Nuclear Physics Laboratory for its hospitality and the NCSR Demokritos for financial support, during my sabbatical leave.

[1] J. A. Wheeler, Phys. Rev. **52**, 1083 (1937).
[2] W. Wefelmeier, Z. Phys. **107**, 332 (1937).
[3] D. Dennison, Phys. Rev. **57**, 454 (1940).
[4] D. Dennison, Phys. Rev. **96**, 378 (1954).
[5] S. L. Kameny, Phys. Rev. **103**, 358 (1956).
[6] D. M. Brink, in *The Alpha-Particle Model of Light Nuclei,* Proceedings of the International School of Physics, "Enrico Fermi," Course XXXVI, edited by C. Bloch (Academic, New York, 1966).
[7] D. M. Brink, H. Friedrich, A. Weiguny, and C. W. Wong, Phys. Lett. **33B**, 143 (1970).
[8] D. Robson, Phys. Rev. Lett. **42**, 876 (1979).
[9] D. Robson, Phys. Rev. C **25**, 1046 (1984).
[10] W. Bauhoff, H. Schultheis, and R. Schultheis, Phys. Lett. **95B**, 5 (1980); **106B**, 278 (1981); Phys. Rev. C **22**, 861 (1980); **29**, 1046 (1984).
[11] S. Marsh and W. D. M. Rae, Phys. Lett. B **180**, 185 (1986).
[12] W. D. M. Rae and A. C. Merchant, Mod. Phys. Lett. A **8**, 2435 (1993); J. Zhang and W. D. M. Rae, Nucl. Phys. **A564**, 252 (1993).
[13] A. C. Merchant and W. D. M. Rae, Nucl. Phys. **A549**, 431 (1992).
[14] W. D. M. Rae, A. C. Merchant, and J. Zhang, Phys. Lett. B **321**, 1 (1994).
[15] G. Leander and S. E. Larsson, Nucl. Phys. **A239**, 93 (1975).
[16] N. M. Strutinsky, Nucl. Phys. **122**, 1 (1968).
[17] G. S. Anagnostatos, Int. J. Theor. Phys. **24**, 579 (1985).
[18] G. S. Anagnostatos, Can. J. Phys. **70**, 361 (1992).
[19] W. F. Hornyak, *Nuclear Structure* (Academic, New York, 1975).
[20] G. S. Anagnostatos and C. N. Panos, Phys. Rev. C **26**, 260 (1982).
[21] G. S. Anagnostatos and C. N. Panos, Lett. Nuovo Cimento **41**, 409 (1984).
[22] C. N. Panos and G. S. Anagnostatos, J. Phys. G **8**, 1651 (1982).
[23] G. S. Anagnostatos, Phys. Rev. C **39**, 877 (1989).
[24] G. S. Anagnostatos and C. N. Panos, Phys. Rev. C **42**, 961 (1990).
[25] G. S. Anagnostatos, T. S. Kosmas, E. F. Hefter, and C. N. Panos, Can. J. Phys. **69**, 114 (1991).
[26] E. Merzbacher, *Quantum Mechanics* (Wiley, New York, 1975).
[27] J. Leech, Math. Gaz. **41**, 81 (1957).
[28] G. S. Anagnostatos, Lett. Nuovo Cimento **22**, 507 (1978).
[29] G. S. Anagnostatos, Lett. Nuovo Cimento **28**, 573 (1980).
[30] G. S. Anagnostatos, Lett. Nuovo Cimento **29**, 188 (1980).
[31] G. S. Anagnostatos, J. Yapitzakis, and A. Kyritsis, Lett. Nuovo Cimento **32**, 332 (1981).
[32] C. W. de Jager, H. de Vries, and C. de Vries, At. Data Nucl. Data Tables **14**, 479 (1974).
[33] A. H. Wapstra and N. B. Grove, Nucl. Data Tables **9**, 267 (1971).
[34] F. Ajzenberg-Selove and T. Lauritsen, Nucl. Phys. A**433**, 1 (1985).
[35] R. Hofstadter, *Nuclear and Nucleon Structure* (Benjamin, New York, 1963), p. 308.
[36] H. S. M. Coxeter, *Regular Polytopes*, 2nd ed. (Macmillan, New York, 1963), p. 292.
[37] P. H. Stelson and L. Grodzins, Nucl. Data, Sec. A **1**, 21 (1965).
[38] N. de Takacsy, Nucl. Phys. **A178**, 469 (1972).
[39] A. C. Merchant (private communication).
[40] M. Kamimura, Nucl. Phys. **A351**, 456 (1981); H. Friedrich, L. Satpathy, and A. Weiguny, Phys. Lett. **36B**, 189 (1971).
[41] H. Friedrich and A. Weiguny, Phys. Lett. **35B**, 105 (1971).
[42] W. J. Vermeer, M. T. Esat, J. A. Kuehner, and R. H. Spear, Phys. Lett. **122B**, 23 (1983).
[43] N. Takigawa and A. Arima, Nucl. Phys. **A168**, 593 (1971).
[44] Y. Abgrall, P. Gabinski, and J. Labarsouque, Nucl. Phys. **A232**, 235 (1974).